Novel Near-Infrared-II In Vivo Visualization Revealed Rapid Calcium Intestine Turnover in Daphnia magna with Delayed Impact by Cadmium and Acidification

Wang, Mengyu; Xie, Huilin; Tang, Ben Zhong; Wang, Wen-Xiong

Published in:
Environmental Science and Technology

Published: 12/03/2024

Document Version:
Post-print, also known as Accepted Author Manuscript, Peer-reviewed or Author Final version

Published version (DOI):
10.1021/acs.est.3c10468

Publication details:
Wang, M., Xie, H., Tang, B. Z., & Wang, W.-X. (2024). Novel Near-Infrared-II In Vivo Visualization Revealed Rapid Calcium Intestine Turnover in Daphnia magna with Delayed Impact by Cadmium and Acidification. *Environmental Science and Technology*, *58*(10), 4558-4570. https://doi.org/10.1021/acs.est.3c10468

Novel Near-Infrared-II *In vivo* Visualization Revealed Rapid Calcium Intestine Turnover in *Daphnia magna* with Delayed Impact by Cadmium and Acidification

Mengyu Wang[1,2$], Huilin Xie[3$], Ben Zhong Tang[3,4], Wen-Xiong Wang[1,2]*

[1]*School of Energy and Environment, State Key Laboratory of Marine Pollution, City University of Hong Kong, Kowloon, Hong Kong, China*

[2]*Research Centre for the Oceans and Human Health, City University of Hong Kong Shenzhen Research Institute, Shenzhen 518057, China*

[3]*Department of Chemistry, Hong Kong Branch of Chinese National Engineering Research Center for Tissue Restoration and Reconstruction, The Hong Kong University of Science and Technology (HKUST), Clear Water Bay, Kowloon, Hong Kong, 999077 China*

[4]*School of Science and Engineering, Shenzhen Institute of Aggregate Science and Technology, The Chinese University of Hong Kong, Shenzhen (CUHK-Shenzhen), Guangdong 518172, China*

$ Mengyu Wang and Huilin Xie contributed equally to this paper.

*Corresponding author, Email: wx.wang@cityu.edu.hk

ABSTRACT

Calcium is a highly demanded metal, and its transport across the intestine of *Daphnia magna* remains a significant unresolved question. Due to technical constraints, the visualization of the kinetic process of Ca passage through *D. magna* has been challenging. Here, we developed the second near-infrared Ca sensor (NIR-II Ca) and conducted real-time *in vivo* imaging of Ca in daphnids with a high signal-to-noise ratio, deep tissue penetration, and minimal damage. Through the utilization of the NIR-II Ca sensor, we for the first time visualized and quantified the kinetic process of Ca passage in the intestine in real-time. The results revealed that trophically available Ca passed through the intestines in 24 h, whereas waterborne Ca required only 35 min. This rapid "flushing through" mechanism established waterborne Ca as the primary source of Ca absorption. However, environmental stressors such as water acidification and cadmium significantly delayed the Ca passage and absorption. The development of NIR imaging and sensors allows for real-time dynamic visualization of contaminants/nutrients in organisms and holds great potential as a powerful tool for future studies into material kinetic processes in living animals.

KEYWORDS: Ca passage; Near-Infrared-II imaging; Ca sensor; acidification; cadmium

One sentence synopsis: Novel second near-infrared Ca sensor imaging in daphnids revealed the rapid "flushing through" mechanism of waterborne Ca impeded by water acidification and cadmium.

GRAPHICAL ABSTRACT (created by the authors)

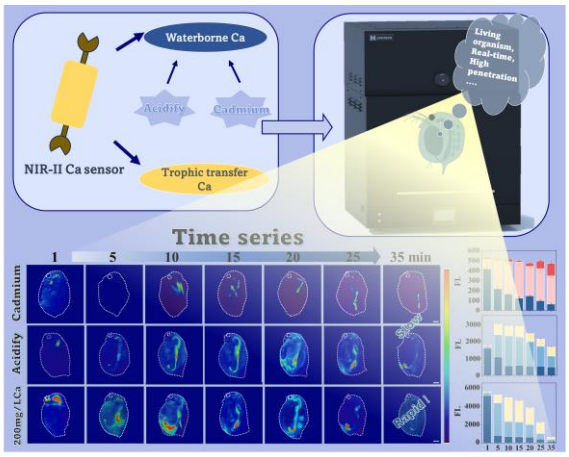

INTRODUCTION

Calcium (Ca) uptake and cycling are critical for freshwater organisms.[1] Bone and shell formation in freshwater organisms rely on Ca absorption and cycling.[2] The uptake and cycling of Ca ensure the maintenance of appropriate cellular Ca^{2+} concentrations, thereby supporting normal metabolic reactions.[3] Besides, Ca uptake and cycling contribute to the nutrient cycling of freshwater organisms. Primary organisms pass Ca to higher-level organisms through Ca uptake in the food chain.[4] The intestine serves as the primary site for Ca^{2+} absorption,[5] making it crucial to understand the mechanisms underlying Ca absorption in aquatic animals.

Daphnia magna (*D. magna*) is a crucial zooplankton species in freshwater environments and serves as a well-established model organism, which has significantly higher Ca requirements than other aquatic organisms.[6,7] *D. magna* required high levels of Ca from the surrounding medium to support regular molting, development, reproduction, and other physiological functions.[8] Within *D. magna*, Ca was primarily distributed in the exoskeleton in the form of carbonates and phosphates.[9] It was reported that Ca concentration of *D. magna* increased with the Ca contents in the aqueous environment. [12] Under low Ca conditions, *D. magna* adapted by producing a thinner carapace, delaying reproduction, and reducing body size as a survival strategy; however, these adaptations increased their susceptibility to mechanical damage and predation.[10, 11] In aquatic ecosystems, *D. magna* occupies a crucial position near the bottom of the food chain, dominating the first level of consumption and serving as the major energy source for numerous secondary consumers.[12] Consequently, *D. magna* plays a pivotal role in upholding ecosystem stability and transferring nutrients throughout the food web.[7] When water Ca concentration decreased, the overall Ca levels in *D. magna* also declined. This in turn resulted in a significant reduction in *D. magna* populations, thereby influencing the stability of the ecological chain.[13] The Ca concentration in *D. magna* reached levels as high as 2.24% of the dry weight, with a residence time of 2 to 55 min in *D. magna* gut.[14, 15] These findings indicated an exceptional efficiency in the absorption and assimilation of Ca by *D. magna*, meeting its elevated Ca demands. However, the mechanisms of intestinal Ca absorption in *D. magna* remain unresolved, necessitating a comprehensive understanding of intestinal dynamics.

In addition, environmental stressors such as acidification and metal Cd can impede the Ca uptake by *D. magna*. The recent rise in atmospheric CO_2 has led to increased uptake of CO_2 by the global oceans, resulting in elevated acidification levels of water bodies.[16, 17] Although the initial period after water acidification may be beneficial to increase the

bioavailable Ca, the long-term effects can result in the loss of Ca from the organisms, e.g., dissolution of $CaCO_3$ as the main component of hard structure.[18] It has been reported that a 1.5 unit decrease in water pH directly affected *D. magna* calcification in the form of reduced body size, growth rate and calcification.[19] Various studies showed that the presence of Cd inhibited Ca uptake by *D. magna*, which interfered with growth and metabolism.[20, 21] Most studies focused on the acute toxicity of Cd to *D. magna* under different Ca or pH conditions, whereas understanding of the kinetics of Ca uptake was very limited. Therefore, how acidification and Cd affected the Ca passage through the intestine of *D. magna* is also an important research gap, which is essential for the study of the mechanisms of Ca uptake as well as the survival of *D. magna* populations.

Previous studies of Ca kinetic processes mainly relied on concentration measurements and radioisotopes. However, the concentration measurement method only provides insights at a specific time point and overlooks the intermediate kinetic processes.[7] The radioisotope method can provide information on Ca movement and metabolic processes in organisms,[22] but falls short in providing detailed information on localized Ca dynamics within tissues. Additionally, radioisotopes require extended tracking periods, making it challenging to capture rapid changes in Ca dynamics over short durations.[23] The radioactivity and toxicity of radioisotopes may also lead to health risks.[24] Due to these methodological limitations, a research gap remains in the understanding of Ca dynamics, especially when the intestine is subdivided into foregut, midgut, and hindgut.[25] Environmental parameters such as pH also exert significant impacts on intestinal Ca absorption, but conventional measurement tools commonly restrict their assessment. Even though some commercial visible region sensors have been employed to detect Ca in small organisms and cells,[26] several limitations hinder their widespread applications, including autofluorescence of the organisms, interference from high background fluorescence signals, elevated detection limits, and the occurrence of false-positive results.[27, 28]

To address the aforementioned challenges, we synthesized and utilized for the first time a second near-infrared region Ca (NIR-II Ca) sensor with aggregation-induced emission (AIE) properties. This novel approach enables *in vivo* real-time kinetic localization and quantification of Ca^{2+} in the intestine. The *in vivo* NIR fluorescence imaging represents an emerging biomedical imaging technique with well-established safety and methodology.[29, 30] Compared to other methods for biological tissue imaging, NIR imaging offers substantial advantages. One notable advantage of NIR imaging is non-ionizing radiation, which eliminates the risk of tissue damage, thereby enabling the possibilities of kinetic imaging.[31, 32]

The longer wavelengths of NIR fluorescence result in reduced light scattering and biomolecular absorption and can penetrate deep into tissues.[33, 34] In addition, NIR imaging also benefits from the low autofluorescence exhibited by biological tissues at long wavelengths, ensuring a high signal-to-noise ratio within the organism.[34, 35] Over the past decade, NIR fluorescence imaging has focused on traditional NIR-I imaging (700-900 nm), while recent advances have been made in the field of NIR-II imaging (1000-1700 nm).[36, 37] By further reductions in scattering, absorption, and organismal autofluorescence, *in vivo,* NIR-II fluorescence imaging outperforms imaging in NIR-I imaging capabilities.[38-41] NIR-II imaging has been used for medical diagnosis, tumor therapy, and photothermal imaging.[42, 43] However, near-infrared two-region sensors with stimulus-responsive properties are lacking, and such sensors are seldom applied to the detection of environmental substances.

In this study, we developed and applied a novel NIR-II Ca sensor to visualize and quantify the kinetic processes of Ca^{2+} in the intestine of *D. magna*, enabling for the first time the imaging of the kinetic processes of Ca^{2+} passage in the intestine. The NIR-II Ca^{2+} sensor quantified the Ca absorption and depuration through both waterborne uptake and trophic transfer *in vivo*. In addition, the sensor exhibits sensitivity to Ca in acidic environments, which allows the detection of Ca in the organism's intestine, providing a powerful tool for investigating the kinetics of Ca passage in *D. magna* intestine. We also explored changes in Ca kinetics in *D. magna* intestine under environmental stresses of acidification and Cd. The NIR-II sensor exhibited minimal damage to living animals and penetrated thicker biological tissues, serving as a powerful tool for future studies of contaminant kinetics in living animals.

MATERIALS AND METHODS

Production of Near-infrared II Calcium Sensor

Benzobisthiadiazole (BBTD) is a heterocyclic compound known for its strong electron-withdrawing ability.[44] This unique characteristic makes BBTD an excellent foundational component for the creation of near-infrared emissive probes, particularly aggregation-induced emission (AIE) molecules that exhibit vibrant fluorescence.[44] Ethylenediaminetetraacetic acid (EDTA) is a chelating agent widely recognized for its ability to bind with Ca^{2+}.[45] Through coordination with the metal ion via its carboxylate and amine groups, EDTA forms a stable complex with Ca^{2+}. This stable complex formation makes EDTA an ideal candidate for constructing probes containing EDTA and exhibiting AIE characteristics. In our study, we prepared a NIR-II Ca sensor by Suzuki coupling reaction with both NIR-II luminescence and Ca^{2+} recognition ability by introducing Ca^{2+} recognition groups (EDTA) into a skeleton of the

near-infrared emissive AIE molecule. By combining BBTD and EDTA, we successfully developed a molecule capable of modulating its fluorescence intensity in response to changes in Ca^{2+} concentration. We then performed serial characterizations of the sensor, including changes in photoluminescence with pH, temperature, and Ca^{2+} concentration, as well as the photostability of the sensor.

Algal and *D. magna* Culture

The algae (*C. reinhardtii*) were cultured in an artificial Tris-Acetate-Phosphate (TAP) medium with bubbled air and collected at the exponential phase of growth. *C. reinhardtii* were harvested by centrifugation at 2700 rpm for 20 min before use. The supernatant was discarded, and the algae sediment from the bottom was washed and resuspended in SM7 medium (a modified simplified M7 medium, containing 0.04 mM $NaHCO_3$, 0.50 mM $MgSO_4$, 0.05 mM KNO_3, and pH at 7.0−8.0). The concentrated algae cell density was measured using a hemocytometer. To determine the dry weight (dw), the algae were collected by 12000 rpm centrifugation for 5 min. After washing and drying at 105 °C for 24 h, the algae were weighed to obtain the total dry weight.

D. magna were cultured in the creek water in our laboratory for about 20 years and fed with *C. reinhardtii* at a density of 5×10^4 cells/mL daily. The density of *D. magna* was controlled at 1 individual/10 ml. The water temperature was set at 23.5 °C, and the photoperiod was 14 h light/10 h dark. All tests were conducted on 7-day-old *D. magna*, and the media used in the whole experiments was a modified medium (SM7, containing 0.04 mM $NaHCO_3$, 0.50 mM $MgSO_4$, 0.05 mM KNO_3, and pH 7.0-7.5). *D. magna* were acclimated in clean SM7 for 12 h prior to viability testing. 10 individuals were then exposed to a medium containing different concentrations of NIR-II Ca sensor in a beaker containing 100 ml of SM7. After 96 h, the mortality of *D. magna* from different treatments was recorded.

Kinetic Processes of Waterborne Calcium Passage through Intestine of *D. magna*

Firstly, we performed acute toxicity tests for *D. magna* according to the OECD Guidelines for Testing Chemicals No. 202 (OECD, 2004). Twenty 7-day-old *D. magna* were exposed to 200 ml of Ca-free SM7 medium containing 0-200 ug/L of NIR-II Ca sensor. Each treatment contained three replicates. After 96 h, the mortality of *D. magna* was recorded and shown in Figure S1. Freshwater typically has a Ca level ranging from 4-100 mg/L, and due to various production activities, freshwater can become acidified with a pH of 5-7.[46] For *D. magna*, the ecological niche of Ca concentration and freshwater pH can be down to 0.5 mg/L

and 5.75.[20] To determine the passage time of intestinal Ca, *D. magna* were exposed to SM7 containing 0, 20, and 200 mg/L Ca^{2+} ($CaCl_2$), under pH 7 for 2 min. Meanwhile, we set up acidic conditions of pH 5, and 6 and conducted exposure experiments with 20, and 200 mg/L Ca^{2+} concentrations under each acidic condition to investigate the effects of pH and concentration on the passage time of Ca in *D. magna* intestine. After Ca exposure at different concentrations and NIR-II Ca sensor staining (1 mM, working solution 1:100 dilution), *D. magna* were rapidly rinsed with deionized water and then placed in the corresponding pH SM7 solution to image continuously for 40 min using the NIR-II small animal fluorescence imaging system (DeepVision™ Imager, NIRMADAS BIOTECH, USA). *D. magna* were captured during continuous imaging at 1, 5, 10,15, 20, 25, and 35 min, respectively. We also measured the pH of different acidity solutions and used a commercial pH sensor to image the acidity of *D. magna* intestinalis after 5 min exposure using confocal microscopy (LSM 900, ZEISS, Germany) under different Ca concentrations and pH conditions. In addition, to investigate the impact of water acidification on Ca accumulation in the intestine, *D. magna* were exposed to 0, 20, and 200 mg/L Ca^{2+} at pH 5, 6, and 7, respectively, for 48 h to reach accumulation equilibrium. After collection, the intestine of *D. magna* was dissected and measured using ICP-MS (PerkinElmer optima 6000, USA) to determine the Ca concentration. The same procedure was performed for the following *D. magna* exposed to trophic transfer Ca. For the NIR-II Ca sensor, excitation: 808 nm, emission collected: ⩾1100 nm; For the pH sensor, excitation: 488 nm, emission collected: 585-635 nm.

Kinetic Processes of Trophic Transfer Calcium Passage through Intestine of *D. magna*

For the trophic transfer of Ca from algae to *D. magna, C. reinhardtii* with an initial density of 1×10^5 cells/mL were inoculated in 100 mL Ca-free SM7 medium and exposed to 0, 20, and 200 mg/L Ca^{2+} at 24 ℃ and 16 h:8 h light/dark. After 24 h, the cell density of algae was measured with a cell counter. *C. reinhardtii* were centrifuged at 3000 rpm for 10 min and washed to remove the Ca^{2+} attached to the surface. Subsequently, the algae were imaged using a commercial Ca^{2+} sensor (Fluo-4 AM, cell-permeant, ThermoFisher SCIENTIFC) by confocal microscopy (LSM 900, ZEISS, Germany) to explore the Ca distribution in algae. After digestion of the algae with 65% HNO_3, the Ca and P concentrations were determined by ICP-OES (PerkinElmer optima 6000, USA). The algae with different Ca concentrations were then exposed to SM7 medium containing *D. magna* for 5 min at pH 5, 6, and 7, respectively. Then, *D. magna* were removed for staining and washing and continued to be

exposed to clean SM7 medium of the corresponding pH for 24 h. For all treatment groups, *D. magna* were collected for NIR-II Ca sensor imaging at exposure times 0, 2, 5, 8, 11, and 24 h, respectively. After 24 h exposure, *D. magna* were collected to determine the Ca concentration in the gut by ICP-MS. For the NIR-II Ca sensor, excitation: 808 nm, emission collected: ⩾ 1100 nm; For the pH sensor, excitation: 488 nm, emission collected: 585-635 nm; For commercial Ca^{2+} sensor (Fluo-4 AM), excitation: 488 nm, emission collected: 495-525nm.

Kinetics of Calcium Passage through Intestine of *D. magna* after Cadmium Exposure

To investigate the influences of Cd on the passage of Ca through the *D. magna* intestine, we first exposed *D. magna* to 0 (as control), 1, and 5 μg/L Cd for 48 h, respectively. After collection (10 individuals were collected from each treatment group in three replications), the intestines of *D. magna* were dissected and measured using ICP-MS (PerkinElmer optima 6000, USA) to determine the Cd accumulation. The *D. magna* were then washed, exposed to 200 mg/L Ca^{2+} and stained. Sequential imaging of the *D. magna* intestinal was performed over a 40-min period. For the NIR-II Ca sensor, excitation: 808 nm, emission collected: ⩾ 1100 nm.

QA/QC and Statistical Analysis

All data were presented as means and standard deviations. Ca concentrations in *C. reinhardtii* and *D. magna* were reported on a dry weight (dw) basis. In this study, the number of *D. magna* in each treatment (including concentration determination and imaging) was 10 to achieve experimental precision. During Ca analyses using ICP-MS, three replicates were used for each treatment. Images were processed by ZEN 3.5 (blue edition) and Fiji software. All data analyses were performed using SPSS (version 25.0) for one-way analysis of variance (ANOVA) with Bonferroni correction. Figures were created using SigmaPlot (version 14.0, Systat Software Inc., CA). The significance level was set at 5%.

RESULTS AND DISCUSSION

Characterization of Near-infrared II Calcium Sensor

AIE molecules usually displayed weak fluorescence in dilute solutions. However, the fluorescence was significantly enhanced upon aggregate formation.[47-49] Exploiting this property, we designed an NIR emissive AIE sensor with two ligand chelating groups to coordinate Ca^{2+}. In the single-molecule state, the AIE probe exhibited weak luminescence. In

the presence of Ca^{2+}, the sensor underwent chelation and aggregation, resulting in a significant increase in fluorescence intensity (Figure 1a). We combined the BBTD-based AIE molecule with EDTA to construct a responsive compound capable of NIR-II emission upon binding to Ca^{2+}. The BBTD-contained unit can provide the near-infrared II emission and AIE properties, while EDTA can act as a Ca^{2+} chelating unit. The synergistic combination of these two components resulted in the development of a Ca sensor capable of modulating its fluorescence intensity in response to changes in Ca^{2+} concentration. The absorption and emission spectrum of the NIR-II Ca sensor molecule were measured. The absorption spectrum of the Near-infrared II Ca Sensor, as shown in Figure 1b, indicated a maximum absorption at 677 nm. However, it should be noted that the sensor also exhibited absorption at 808 nm, indicating that it can be excited by 808 nm NIR light. Therefore, the sensor was suitable for near-infrared imaging applications (Figure 1c). The emission spectra of this sensor peaked at 935 nm and remained strong up to 1100 nm (Figure 1c). The absorption and emission were in the near-infrared region, which provided the possibility of deeper penetration depths and brighter biological imaging. Notably, the NIR-II Ca sensor exhibited a large Stokes shift of 258 nm, minimizing self-absorption and resulting in a high signal-to-noise ratio, thereby enhancing sensitivity in biological applications. We detected that the photoluminescence intensity of the NIR-II Ca sensor was not significantly affected under different acidity conditions (pH 3~8) and different temperature conditions (5 ℃, 20 ℃, and 40 ℃), illustrating the reliability and generalizability of the sensor under different environmental conditions (Figure 1d, e). We also determined the change of fluorescence intensity of the sensor under different Ca concentration conditions (0, 3.125, 6.25, 12.5, 25, 50, 100, 200, 400 mg/L Ca^{2+}), and found that the fluorescence intensity of the sensor was enhanced with the increase of Ca concentration, and the logarithm of Ca concentration and fluorescence intensity showed a strong linear relationship (R^2= 0.976) (Figure $1f_1$). In addition, the photostability of the sensor performed well after 6 tests under 2W/cm^2 laser (Figure $1f_2$).

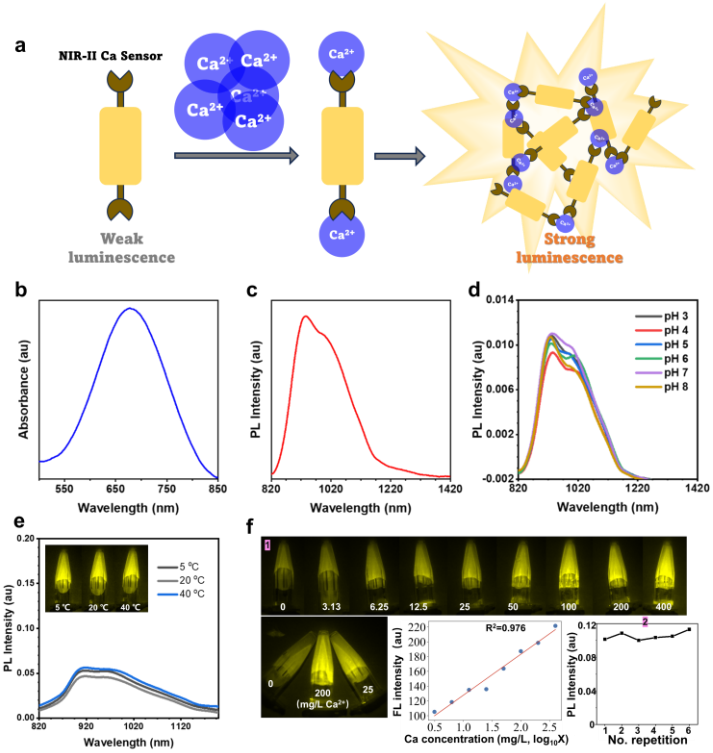

Figure 1. Characterization of Near-infrared II Ca Sensor. (a) Flowchart of NIR-II Ca sensor for detecting Ca^{2+} luminescence. (b) Illustration of absorbance of NIR-II Ca sensor. (c) Illustration of photoluminescence intensity of NIR-II Ca sensor. (d) Photoluminescence intensity of NIR-II Ca sensor under different pH conditions. (e) Photoluminescence intensity of NIR-II Ca sensor under different temperature conditions. (f) Fluorescence intensity changes under different Ca^{2+} concentrations, the linear relationship between the logarithm of Ca concentration and fluorescence intensity, and the photostability of the NIR-II Ca sensor. The color of the image in (e) and (f) is pseudo-color, indicating the signal value.

Real-time Imaging of Waterborne Calcium Passage Kinetics in *D. magna* Intestine

The global median Ca concentration in aqueous environment is 4.0 mg/L, with 20% of water samples exhibiting Ca concentrations below 1.5 mg/L.[50] Ca content of different species of *D. magna* can be as much as 2.24% dry weight.[14] Given their regular molting, *D. magna* has a substantial demand for Ca, and must continuously absorb Ca from the aqueous environment.[51] Numerous evidence suggested that *D. magna* was highly sensitive to low Ca concentrations, and field studies demonstrated reduced population growth in zooplankton species under such conditions.[52] Laboratory studies further revealed that low-Ca environments led to diminished body size, survival rate, and reproductive capabilities in *D. magna*.[1, 53, 54] However, previous studies predominantly focused on the endpoint of accumulation deficiency effects of Ca in the body, while investigations into the kinetics of Ca passage through the intestine were limited.[10, 13, 55] The tiny intestine of *D. magna* consists of the foregut, midgut, and hindgut, with food entering the hindgut from the midgut and being expelled from the anus through peristaltic contractions and pressure from the incoming food

particles.[56] Although some studies explored the intestinal residence time and clearance time of food, there were still significant challenges in understanding how Ca passed through each intestinal structure, which is the basis for investigating how Ca is absorbed and assimilated in the gut. [57, 58, 59] The challenge lies in the fact that the tiny intestine and complex microenvironment of *D. magna* make it difficult to image Ca^{2+} kinetic processes throughout the intestine, even with fluorescence microscopy, due to insurmountable autofluorescence and low signal-to-noise ratios.[60] Additionally, for large-sized *D. magna*, imaging of the intestine may be incomplete due to the limited working distance of ordinary fluorescence microscopes.

In this study, we synthesized and applied a NIR-II Ca sensor for the first time to directly visualize the Ca^{2+} passage through *D. magna* intestine. By this means, we quantified the accumulation and excretion of Ca^{2+} in the foregut, midgut, and hindgut, respectively, providing a theoretical foundation for understanding the digestion kinetics of Ca in the intestine. Initially, we tested the impacts of the NIR-II Ca sensor on the growth of *D. magna* within the range of 10 to 200 μmol/L after 96-h exposure (Figure S1). The results showed that the survival rate of *D. magna* remained above 90% at 200 μmol/L, indicating the excellent biocompatibility of the NIR-II Ca sensor. Subsequently, we visualized the kinetic process of Ca^{2+} passage in *D. magna* intestine under pH 7 and three different Ca concentrations (0, 20, and 200 mg/L). As shown in Figure 2a, the overall process of Ca^{2+} passage through the gut lasted 35 min. Within this timeframe, Ca^{2+} passed through the foregut in approximately 10 min, while the duration was more prolonged within the midgut and hindgut, which are critical for the processes of digestion and absorption.[61]

To further determine the dynamics of Ca^{2+} in the intestine, we quantified the fluorescence intensity of Ca^{2+} during the passage process. The foregut was the beginning part of *D. magna*'s digestive system and is primarily responsible for the ingestion and initial digestion, which processed diet by ingesting, [57] mechanically pulverizing, and secreting digestive enzymes in preparation for the subsequent processes of digestion and absorption.[62] The midgut was the main digestive and absorptive area of *D. magna* digestive system, where complex molecules in diet were further broken down into simpler forms for absorption and utilization.[62] The hindgut was located at the end of the digestive system and its main function was to absorb water and expel waste.[62] Therefore, in this study, we quantified the kinetic process of Ca^{2+} passage through the foregut, midgut, and hindgut.

When considering the exposure concentration, higher levels of Ca^{2+} exposure resulted in increased concentrations of Ca^{2+} in the intestine, accompanied by shorter passage time (Figure 2b). With increasing concentration, Ca^{2+} tended to move more rapidly towards the

hindgut for absorption or excretion. This observation highlighted that low Ca concentrations resulted in delayed passage of Ca^{2+} in the gut, potentially due to increased efficiency in Ca absorption by *D. magna*. Previous studies showed variations in the intestinal residence time of *D. magna*, ranging from 2 to 55 min, with shorter passage times observed at higher food concentrations, consistent with the findings of this study.[63, 64] This study provided the first visual demonstration of the dynamics of Ca^{2+} in *D. magna* intestine, facilitated by the NIR-II Ca sensor, which enabled detailed observation of Ca^{2+} in each segment of the intestine.[65] Within 35 min, Ca^{2+} underwent rapid absorption and excretion, with residence time concentrated in the posterior segment of the intestine. The efficient Ca waterborne passage highlighted the potential for effective Ca utilization by *D. magna*.

To further investigate the process of Ca accumulation in the intestine, we evaluated and quantified the accumulation of Ca^{2+} in *D. magna* by the NIR-II Ca sensor. At 1 min, Ca^{2+} was mainly distributed in the anterior intestine of *D. magna* (Figure 2c, d). In the 20 mg/L Ca treatment, the presence of Ca^{2+} in the anterior intestine was visibly prominent (Figure 2c, d). Following 40 min of exposure, Ca^{2+} in the intestine was mainly concentrated in the middle and posterior segments of the intestine (Figure 2c, d). After 48 h of continuous exposure, Ca^{2+} had permeated throughout the entire intestine. In the case of the 200 mg/L Ca^{2+} treatment, a more intense fluorescence was found in the foregut and hindgut, and the higher accumulation of Ca^{2+} was evenly distributed throughout the intestine (Figure 2c, d). These findings suggested that Ca^{2+} tended to accumulate in the posterior intestine at the beginning and then gradually filled the whole intestine as the concentration and duration of exposure increased.

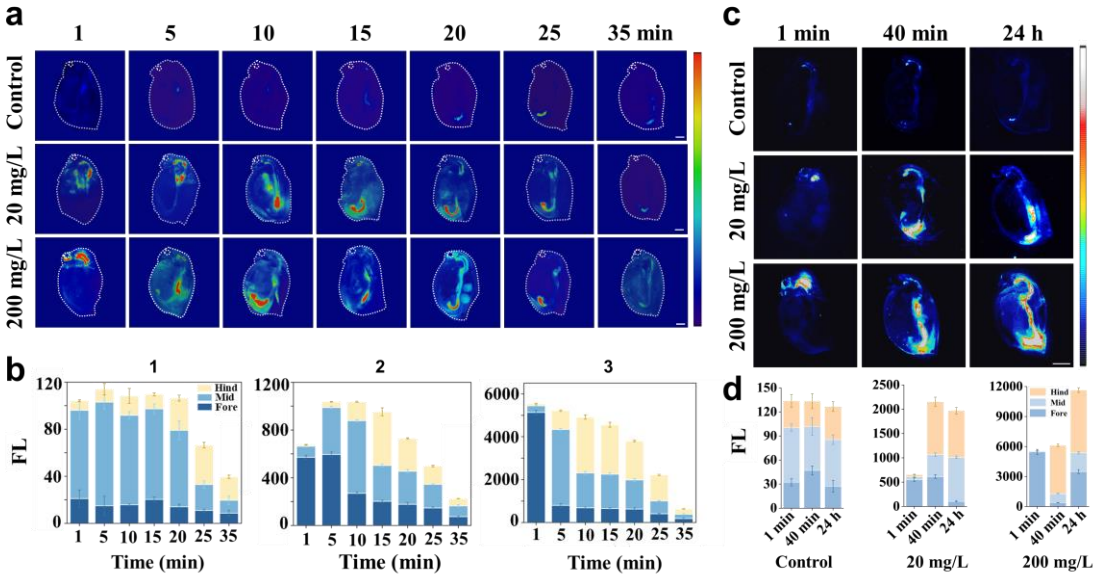

Figure 2. Kinetics of Ca^{2+} uptake in the intestine of *D. magna* via waterborne exposure. (a) NIR images showing the kinetics of Ca^{2+} passage through *D. magna* intestine under different

exposure concentrations. The color bar indicates that the upper color is an area of higher fluorescence intensity. Scale bar: 100 μm. (b) Changes in the fluorescence intensity of Ca^{2+} in the hindgut, midgut, and foregut of *D. magna* during 35 min. Figures b1, b2, and b3 are for the control, 20 mg/L treatment, and 200 mg/L treatment, respectively. (c) NIR images of the distribution of Ca^{2+} accumulation in *D. magna* at different time points at different Ca^{2+} concentrations. (d) Changes in the fluorescence intensity of Ca^{2+} accumulated in the hindgut, midgut, and foregut of *D. magna* after 1min, 40 min, and 24 h continous exposure. Scale bar: 200 μm.

Real-time Imaging of Trophically Available Calcium Passage Kinetics in Intestine

Apart from the ionic state of Ca in the medium, the NIR-II Ca sensor effectively detected trophic transfer Ca, which represented another mechanism of Ca uptake by *D. magna*.[22] In this part, *D. magna* were exposed to altered Ca concentrations of algae. The 0, 20, and 200 mg/L Ca^{2+} were first exposed to *C. reinhardtii* to determine the Ca accumulation, then *C. reinhardtii* were fed to *D. magna,* and the intestine was collected and measured (Figure 3a). Figure 3b shows that Ca^{2+} was detected in the algal cells which overlapped with the distribution of autofluorescence, indicating the accumulation and internalization of Ca^{2+} in the algae (Figure 3b, box). Detectable Ca^{2+} *in vivo* increased with increasing Ca exposure concentrations (Figure 3b). After determination, the Ca level of *C. reinhardtii* exposed to 20 and 200 mg/L Ca^{2+} was higher than the control group (Figure 3c). These indicated that elevated Ca levels in the aquatic environment promote Ca accumulation in algae.

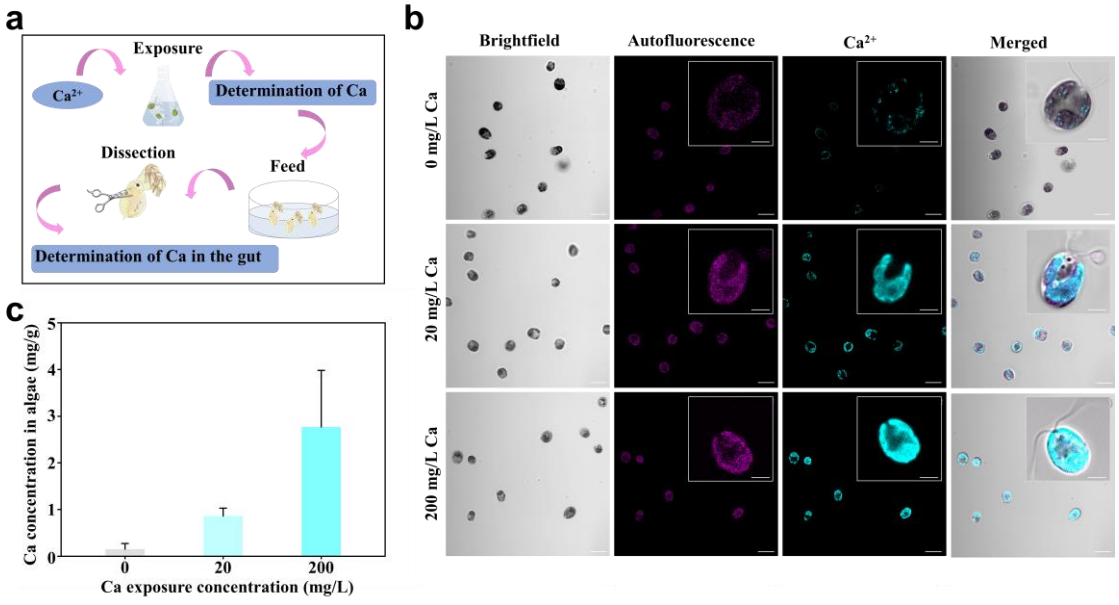

Figure 3. Accumulation and distribution of Ca in algae. (a) Diagram of Ca uptake by algae and trophic transfer to *D. magna*. (b) Imaging of algae after exposure to 0, 20, and 200 mg/L Ca^{2+}. Images showing the bright field, the autofluorescence of algae, the Ca^{2+} channel, and merged. (c) Ca accumulation in algae after exposure to 0, 20, and 200 mg/L Ca^{2+}. Scale bar: 10 μm for normal size and 1μm for box.

C. reinhardtii with different Ca concentrations were then exposed to *D. magna* under pH 7 for 10 min, respectively. We then rapidly transferred *D. magna* to an SM7 medium and imaged the trophic transfer Ca in the intestine by the NIR-II Ca sensor. To capture the passage of trophic transfer Ca through the foregut, midgut, and hindgut of the intestine, we selected representative time points for imaging, i.e., 0, 2, 5, 8, 11, and 24 h after exposure to Ca in *D. magna*. It was found that trophic transfer Ca was excreted *in vivo* after 24 h (Figure 4a), which was distinguishable from waterborne Ca exposure. This suggested that trophic transfer Ca and waterborne Ca were probably absorbed by different mechanisms in the intestine of *D. magna*. By quantifying the fluorescence intensity, it was found that Ca tended to be rapidly transferred to and excreted from the midgut and hindgut as the concentration increased. After 24 h, the residual Ca in the intestine was significantly lower in the high-concentration treatment group compared to the low-concentration treatment group (Figure 4b). This outcome supported the notion that waterborne Ca served as the primary source of Ca, while the contribution of trophic transfer Ca was relatively minor.[55] Considering that calcification in *D. magna* was completed within 24-48 h after molting, it was difficult to consume sufficient Ca through diet to meet the calcification requirements.[55]

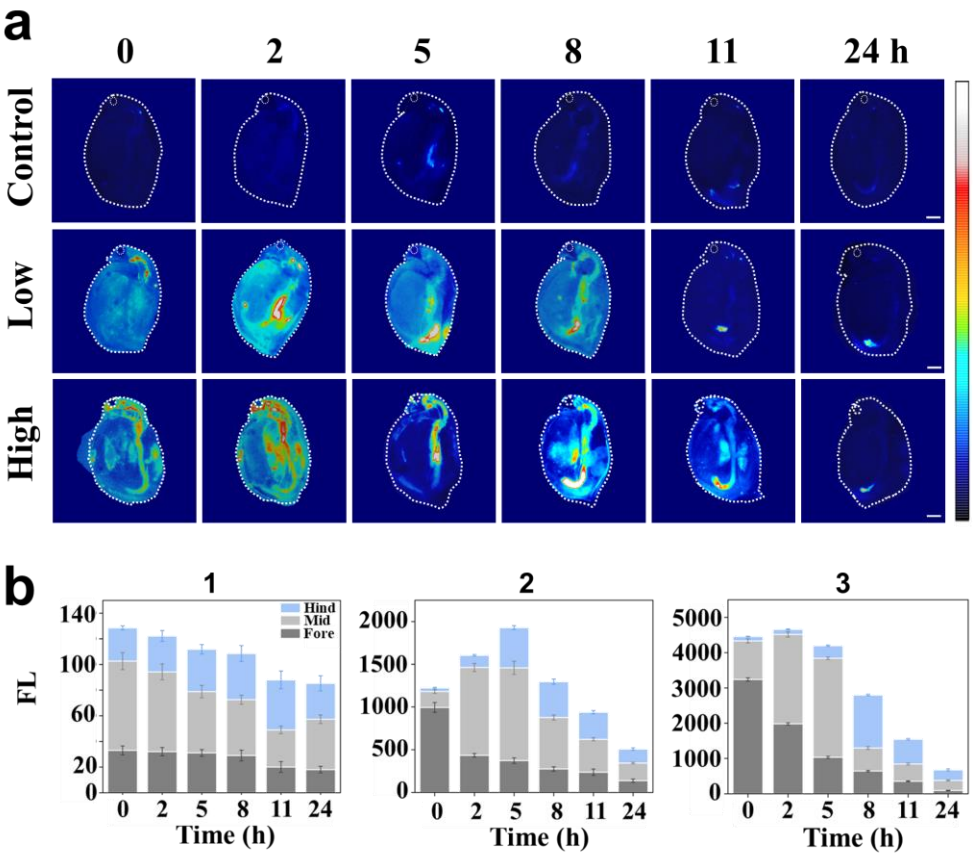

Figure 4. Kinetics of trophic transfer Ca uptake in the intestine of *D. magna*. (a) NIR images showing the kinetics of trophic transfer Ca passage through *D. magna* intestine under different exposure concentrations. The color bar indicates that the upper color is an area of higher fluorescence intensity. Scale bar: 100 μm. (b) Changes in the fluorescence intensity of trophic transfer Ca in the hindgut, midgut, and foregut of *D. magna* during 24 h. Figures b1, b2, and b3 are for the control, low Ca algae exposure treatment, and high Ca algae exposure treatment respectively.

NIR-II Ca Imaging its Kinetic Passage through *D. magna* Intestine under Acidic Conditions

The aquatic environment, both inside and outside the bodies of aquatic organisms, is predominantly characterized by acidity.[66] In addition to the aforementioned factors, we also imaged Ca in *D. magna* under acidic conditions. We combined the NIR-II Ca sensor with a pH sensor to reveal variations in the passage of Ca^{2+} through the intestine under different acidic environments. As shown in Figure 5a, the intestinal acidity of *D. magna* was observed after 3 min of exposure to different conditions. Figure 5b demonstrated that an intensified acidic exposure environment led to higher levels of acidity detected in the intestine of *D. magna*, with a tendency to accumulate in the anterior intestine. The distribution pattern of acidity in *D. magna* intestine exhibited similarity across different conditions of Ca concentration exposure.

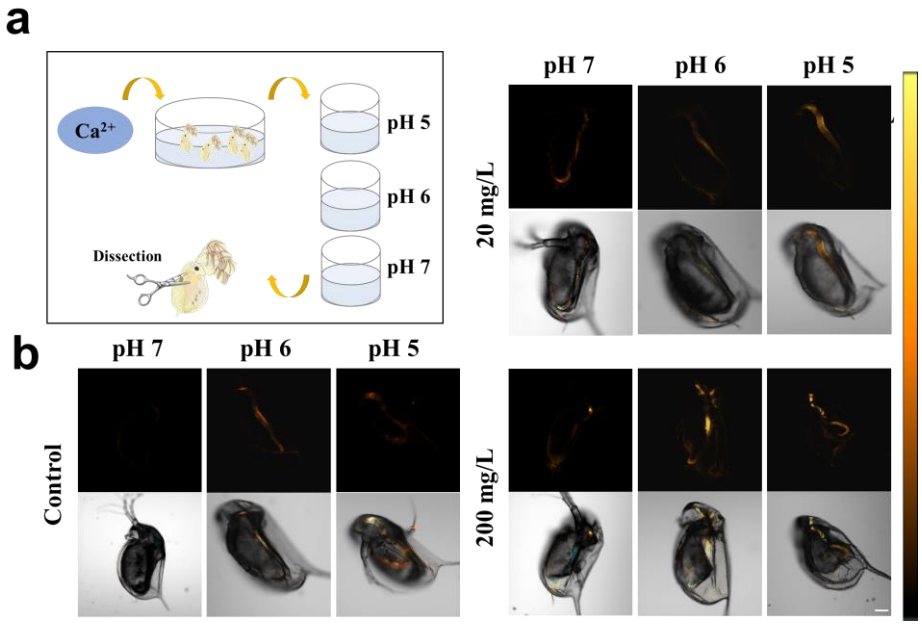

Figure 5. Acidity in the intestine of *D. magna* under different pH conditions. (a) Diagram of waterborne Ca^{2+} exposed to *D. magna* under different pH conditions. (b) Confocal images showing the distribution of acidity in the intestine of *D. magna* under pH 5, 6, and 7 and 0, 20, 200 mg/L Ca^{2+}. The color bar indicates that the upper color is a more acidic region. Scale bar: 100 μm.

Having established that external acidity regulated the pH within the intestine of *D. magna*, we used the NIR-II Ca sensor to visualize the kinetic process of Ca^{2+} passage in *D. magna* intestine under pH 6 and pH 7 conditions. More Ca remained in the intestines after 35 min at pH 5 compared to pH 6 and the neutral conditions mentioned earlier (Figure 6a). Quantification of fluorescence intensity revealed that an acidic exposure environment resulted in a delayed passage of Ca^{2+} throughout the intestine, particularly in the mid-intestine (Figure 6b). Under pH 7 exposure, Ca^{2+} in the foregut rapidly transferred to the midgut and hindgut, subsequently being excreted (Figure 2b). However, as the pH decreased, the transfer of Ca^{2+} from the foregut to the midgut and hindgut became slower, resulting in the persistence of significant Ca levels in the intestines even after 35 min (Figure 6b).

To further investigate the impact of acidification on Ca accumulation in the intestine, *D. magna* was exposed to 0, 20, and 200 mg/L Ca^{2+} at pH 5, 6, and 7 for 48 h, and then Ca concentrations were measured at equilibrium Ca^{2+} in the intestine. For the control group, there was no significant difference in Ca accumulation in the intestine under different pH conditions (Figure 6c), which suggested that in an aqueous environment lacking Ca^{2+}, *D. magna* maintained similar concentrations of intestinal Ca in various acidity environments. However, after treatment with 200 mg/L of Ca^{2+}, intestinal Ca accumulation in *D. magna* exposed to pH 5 was significantly lower than that in pH 7 (Figure 6c). The results indicated that acidification of the aqueous environment inhibited the Ca accumulation in the intestine of *D. magna*. Then, the kinetics of Ca concentration in the intestine were measured during uptake and depuration with 20 mg/L Ca^{2+} exposure at pH 5, 6, and 7. During absorption, intestinal Ca concentration in *D. magna* was lower when exposed to a high-acidity medium and did not reach equilibrium after 48 h of exposure to acidic conditions at pH 5 (Figure 6d). Thus, the acidic environment reduced the accumulation and rate of Ca absorption in the intestine. During depuration, the *D. magna* intestine under pH 5 exhibited a slower depuration rate and less expulsion (Figure 6d), which suggested that acidification of the aqueous environment inhibited Ca activity and accumulation in the *D. magna* intestine throughout both the uptake and depuration phases.

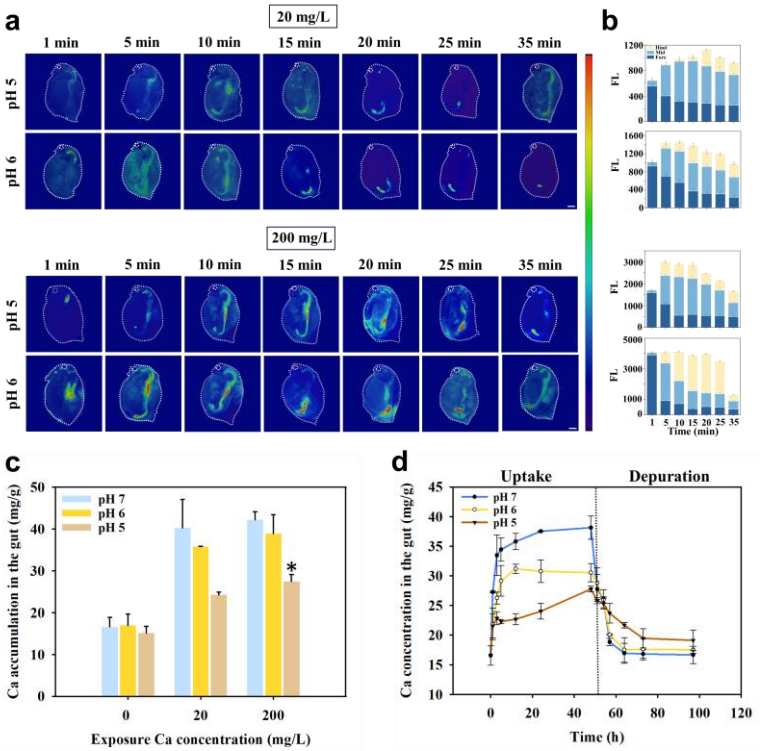

Figure 6. Kinetics of Ca^{2+} uptake in the intestine of *D. magna* under different acidity conditions via waterborne exposure. (a) NIR images showing the kinetics of Ca^{2+} passage through *D. magna* intestine under different pH conditions. The corresponding quantitative results were presented in the same row. The color bar indicates that the upper color is an area of higher fluorescence intensity. Scale bar: 100 μm. (b) Changes in the fluorescence intensity of Ca^{2+} in the hindgut, midgut, and foregut of *D. magna* during 35 min. (c) Waterborne Ca accumulated in the intestine of *D. magna* after 48 h waterborne Ca exposure under pH 5, 6, and 7, respectively. (d) Uptake and depuration time points of Ca^{2+} in the intestine of *D. magna*. Data are mean ± SD. *$p < 0.05$ compared with control.

Apart from the waterborne Ca, the NIR-II Ca sensor can also identify the passage of trophic transfer Ca under low pH conditions in the intestine. We exposed algae to Ca and then fed the algae with different Ca concentrations to *D. magna* under pH 5, 6, and 7 (control) for a duration of 10 min, respectively. Subsequently, we rapidly transferred *D. magna* to an SM7 medium of the corresponding pH and imaged the trophic transfer Ca in the intestine by the NIR-II Ca sensor. Figure 7a showed that the passage of trophic transfer Ca through the intestine was delayed with decreasing pH. Under the same pH condition, the residence time of Ca in the midgut decreased as the concentration increased. For instance, after 8 h at pH 5, the low-Ca treatment resulted in Ca accumulation in the midgut, while the high-Ca exposure led to Ca reaching the posterior portion of the intestines for excretion. By quantifying the fluorescence intensity of detected Ca, we found that the kinetic pattern of trophic transfer Ca through *D. magna* intestine was similar to that of waterborne exposure. In a pH 7 environment, a substantial Ca from the foregut to the midgut and hindgut was observed after

5 h (Figure 4b). After 24 h, a notable reduction in detectable Ca within the intestine was observed (Figure 4b). However, with the acidification of the environment, the transfer of Ca in the intestine decelerated, and large quantities of Ca were still present in the intestine after 24 h without being excreted or absorbed (Figure 7b). This could be attributed to the changes in the transport mechanisms or biochemical processes involved in Ca absorption and excretion.[67, 68] The presence of a large amount of Ca in the intestine after 24 h, without it being excreted or absorbed, indicated a disruption in the normal Ca passage, i.e., acidification of the aqueous environment impeded the efficient digestion and absorption of Ca in the gut. The accumulation of Ca in the intestine under acidic conditions may have implications for the overall Ca balance and nutritional status of the organism.[69, 70] These findings suggested that environmental acidification can interfere with the proper utilization and regulation of Ca, an essential mineral for various physiological processes. We presented the first attempt to visualize the mechanism of Ca passage in the intestine and the inhibition of Ca absorption caused by acidification by combining the NIR-II Ca sensor with the pH sensor, providing valuable insights into the direct visualization of these processes.

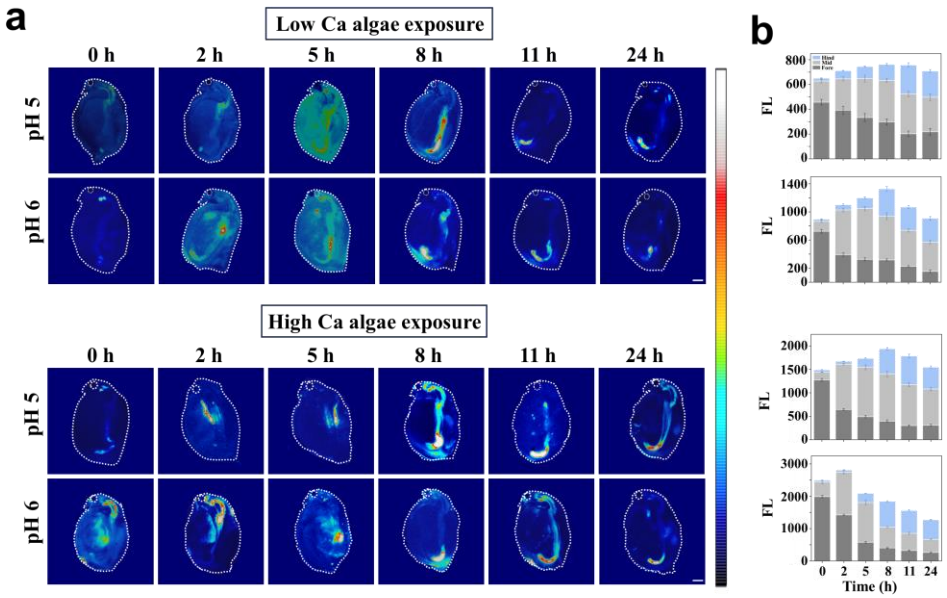

Figure 7. Kinetics of trophic transfer Ca uptake in the intestine of *D. magna*. (a) NIR images showing the kinetics of trophic transfer Ca passage through *D. magna* intestine under different pH conditions. (b) Changes in the fluorescence intensity of trophic transfer Ca in the hindgut, midgut, and foregut of *D. magna* during 24 h. The corresponding quantitative results were presented in the same row. The color bar indicates that the upper color is an area of higher fluorescence intensity. Scale bar: 100 μm.

We then determined the intestinal Ca accumulation in *D. magna* exposed continuously to trophic transfer Ca for 48 h. The results showed that Ca accumulation in the intestine of *D.*

magna fed with 200 mg/L Ca-exposed algae was significantly reduced at pH 5 and pH 6. In the other two groups, *D. magna* intestinal Ca accumulation also showed a tendency to reduce under acidic conditions although there was no significant decrease in Ca accumulation (Figure S2). This indicated that Ca accumulation in the intestine of *D. magna* can be improved by increasing the trophic transfer level of Ca.

NIR-II Ca Imaging its Kinetic Passage through *D. magna* Intestine after Cadmium Exposure

We further explored the kinetic changes of Ca in the intestine of *D. magna* under the influence of Cd. Before imaging, we exposed the *D. magna* to different concentrations of Cd^{2+} for 48 h to equilibrate the Cd content in the body. The *D. magna* were then transferred to 200 mg/L Ca^{2+} and then placed in SM7 solution to image Ca^{2+} in *D. magna* intestine at intervals. After 1 and 5 μg/L Cd exposure (actual concentrations of 0.96±0.01 and 4.18±0.02 μg/L), Cd levels in the intestine of *D. magna* reached 15.64±3.16, 41.91±4.50 μg/g, respectively (Figure 8a); both of which were significantly higher than those in the control group (0.02±0.01 μg/g), suggesting that Cd exposure increased the accumulation of intestinal Cd of *D. magna*. The results of kinetic imaging of Ca results indicated a notable reduction in the influx of Ca into the intestine as Cd exposure concentrations increased, coupled with an extended passage time of Ca through each part of the intestine (Figure 8b). Following the quantification of intestinal Ca fluorescence intensity, at Cd exposure of 5 μg/L, the Ca that passed through the whole intestine to reach the hindgut was not significantly different from the initial Ca (Figure 8c). This observation implied a diminished intestinal capacity to absorb Ca in the presence of Cd, presumably as a result of competitive inhibition and Cd toxicity.[71, 72] As ambient Ca levels increased from 0.5 mg/L to 200 mg/L, Ca accumulation in *D. magna* increased from 0.91% to 3.75%, and the dissolved uptake rate constant of Cd decreased ninefold.[73] There was also a possibility that Cd exposure caused toxicity that affected the normal physiological metabolic processes of *D. magna*, resulting in reduced Ca absorption.[74]

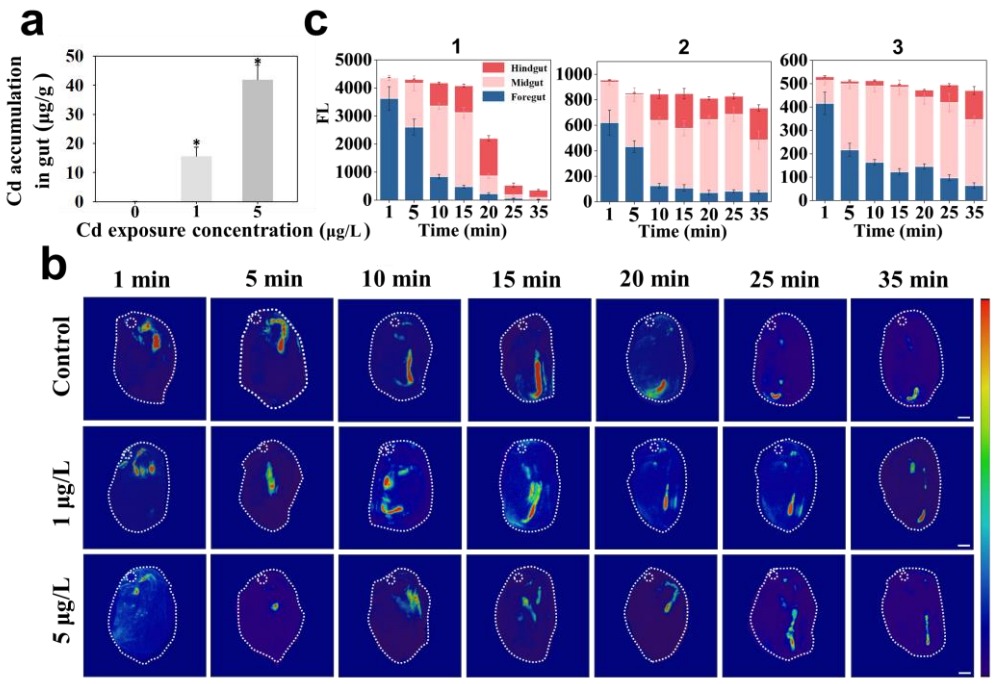

Figure 8. Kinetics of Ca^{2+} uptake in the intestine of *D. magna* under Cd exposure. (a) Cd accumulation in *D.magna* after exposure to 0, 1, and 5 μg/L Cd^{2+} for 48 h. Data are mean ± SD. *$p < 0.05$ compared with control. (b) NIR images showing the kinetics of Ca^{2+} passage through *D. magna* intestine after Cd exposure. The color bar indicates that the upper color is an area of higher fluorescence intensity. Scale bar: 100 μm. (c) Changes in the fluorescence intensity of Ca^{2+} in the hindgut, midgut, and foregut of *D. magna* during 35 min. Figure c1, c2, and c3 are for the control, 1, and 5 μg/L Cd treatment, respectively.

Overall, we developed a novel NIR-II Ca sensor enabling direct imaging and quantification of the kinetic processes of Ca in *D. magna* intestine. It represented the first successful application of a NIR-II detector for ion detection. By utilizing the NIR-II region imaging, we overcame the limitations of commercial sensors, which were prone to organism autofluorescence, interference from high background fluorescence signals, and false positive results during detection. The NIR-II Ca sensor exhibited outstanding properties, including deep tissue penetration and non-invasiveness, enabling real-time tracking of the kinetic processes of Ca within living organisms. We found that waterborne Ca passing through the intestine was absorbed by *D. magna* intestine within 35 min in a rapid "flushing through" mechanism, whereas this process lasted for 24 h for trophic transfer Ca, thus waterborne Ca was the main Ca source for *D. magna*. In both waterborne Ca and trophic transfer Ca, intestinal Ca tended to be rapidly absorbed and excreted through the midgut and hindgut as the Ca concentration increased. Furthermore, despite the rapid passage of waterborne Ca, acidification delayed the passage of Ca through the intestine, and Cd contributed to a

diminished intestinal capacity to absorb Ca, which provided potential ideas for Ca supplementation. Our successful application of the NIR-II sensor to visualize and quantify Ca not only clarified the passage mechanism of Ca dynamics in organisms but also provided a new perspective for the kinetic study of metal ions. Notably, the NIR technology holds promise as a powerful tool for future investigations into contaminant dynamics in living animals, allowing for the dynamic and real-time detection of pollutant/nutrient kinetic processes *in vivo*, rather than being limited to single-time point determination.

ACKNOWLEDGEMENT

We thank the anonymous reviewers for their comments. This study was supported by the Hong Kong Research Grants Council (C6014-20W).

Supporting Information

Survival of *D. magna* exposed to the range of 10 to 200 μmol/L NIR-II Ca^{2+} concentrations; Trophic transfer Ca accumulated in the intestine of *D.magna* after 48 h exposure under pH 5, 6, and 7, respectively.

REFERENCES

1. Huang, J.; Xu, X.; Li, D.; Sun, Y.; Gu, L.; Zhang, L.; Lyu, K.; Yang, Z., Decreased calcium concentration interferes with life history defense strategies of Ceriodaphnia cornuta in response to fish kairomone. *Limnology and Oceanography* **2021,** *66*, (8), 3237-3252.
2. Bilezikian, J. P., Raisz, L. G., & Martin, T. J. (Eds.). **2008**. Principles of bone biology. *Academic press.*
3. Rossi, A.; Pizzo, P.; Filadi, R., Calcium, mitochondria, and cell metabolism: A functional triangle in bioenergetics. *Biochimica et Biophysica Acta (BBA) - Molecular Cell Research* **2019,** *1866*, (7), 1068-1078.
4. Jeziorski, A.; Yan, N. D.; Paterson, A. M., The widespread threat of calcium decline in fresh waters. *Science* **2008,** *322*, (5906), 1374-1377.
5. Shkembi, B.; Huppertz, T., Calcium absorption from food products: Food matrix effects. *Nutrients* **2021,** *14*, (1), 180.
6. Hofmann, G. E.; Barry, J. P.; Edmunds, P. J.; Gates, R. D.; Hutchins, D. A.; Klinger, T.; Sewell, M. A., The effect of ocean acidification on calcifying organisms in marine ecosystems: an organism-to-ecosystem perspective. *Annual review of ecology, evolution, and systematics* **2010,** *41*, 127-147.
7. Pérez-Fuentetaja, A.; Goodberry, F., *Daphnia*'s challenge: survival and reproduction when

599 calcium and food are limiting. *Journal of Plankton Research* **2016,** *38*, (6), 1379-1388.
600 8. Ross, A. J.; Arnott, S. E., Similar zooplankton responses to low pH and calcium may
601 impair long-term recovery from acidification. *Ecological Applications* **2022,** *32*, (3), e2512.
602 9. Rogalski, M. A.; Ferah, U., Lake water chemistry and population of origin interact to shape
603 fecundity and growth in Daphnia ambigua. *Ecology and Evolution* **2023,** *13*, (6), e10176.
604 10. Hessen, D. O.; Alstad, N. E.; Skardal, L., Calcium limitation in Daphnia magna. *Journal*
605 *of Plankton Research* **2000,** *22*, (3), 553-568.
606 11. Riessen, H. P.; Linley, R. D.; Altshuler, I.; Rabus, M.; Söllradl, T.; Clausen-Schaumann,
607 H.; Laforsch, C.; Yan, N. D., Changes in water chemistry can disable plankton prey defenses.
608 *Proceedings of the National Academy of Sciences* **2012,** *109*, (38), 15377-15382.
609 12. Miner, B. E.; De Meester, L.; Pfrender, M. E.; Lampert, W.; Hairston, N. G., Jr., Linking
610 genes to communities and ecosystems: Daphnia as an ecogenomic model. *Proceedings of the*
611 *Royal Society B: Biological Sciences* **2012,** *279*, (1735), 1873-82.
612 13. Muyssen, B. T.; De Schamphelaere, K. A.; Janssen, C. R., Calcium accumulation and
613 regulation in *Daphnia magna*: Links with feeding, growth and reproduction. *Comparative*
614 *Biochemistry and Physiology Part A: Molecular & Integrative Physiology* **2009,** *152*, (1), 53-
615 57.
616 14. Tan, Q. G.; Wang, W. -X., Interspecies differences in calcium content and requirement in
617 four freshwater cladocerans explained by biokinetic parameters. *Limnology and*
618 *Oceanography* **2010,** *55*, (3), 1426-1434.
619 15. Gillis, P. L.; Chow-Fraser, P.; Ranville, J. F., *Daphnia* need to be gut-cleared too: the
620 effect of exposure to and ingestion of metal-contaminated sediment on the gut-clearance
621 patterns of *D. magna*. *Aquat Toxicol* **2005,** *71*, (2), 143-54.
622 16. Gao, K.; Beardall, J.; Häder, D.-P.; Hall-Spencer, J. M.; Gao, G.; Hutchins, D. A., Effects
623 of ocean acidification on marine photosynthetic organisms under the concurrent influences of
624 warming, UV radiation, and deoxygenation. *Frontiers in Marine Science* **2019,** *6*, 322.
625 17. Peters, G. P.; Andrew, R. M.; Boden, T.; Canadell, J. G.; Ciais, P.; Le Quéré, C.; Marland,
626 G.; Raupach, M. R.; Wilson, C., The challenge to keep global warming below 2 C. *Nature*
627 *Climate Change* **2013,** *3*, (1), 4-6.
628 18. Solan, M.; Whiteley, N., Stressors in the marine environment: physiological and
629 ecological responses; societal implications. *Oxford University Press*: **2016**.
630 19. Ramaekers, L.; Vanschoenwinkel, B.; Brendonck, L.; Pinceel, T., Elevated dissolved
631 carbon dioxide and associated acidification delays maturation and decreases calcification and
632 survival in the freshwater crustacean Daphnia magna. *Limnology and Oceanography* **2023**,
633 *68*, (7), 1624-1635.
634 20. Tan, Q.-G.; Wang, W.-X., Acute toxicity of cadmium in Daphnia magna under different
635 calcium and pH conditions: importance of influx rate. *Environmental science & technology*
636 **2011,** *45*, (5), 1970-1976.

21. Komjarova, I.; Blust, R., Effect of Na, Ca and pH on simultaneous uptake of Cd, Cu, Ni, Pb, and Zn in the water flea Daphnia magna measured using stable isotopes. *Aquatic toxicology* **2009,** *94*, (2), 81-86.
22. Tan, Q.-G.; Wang, W.-X., The regulation of calcium in *Daphnia magna* reared in different calcium environments. *Limnology and Oceanography* **2009,** *54*, (3), 746-756.
23. Beck, A. B.; Bügel, S.; Stürup, S.; Jensen, M.; Mølgaard, C.; Hansen, M.; Krogsgaard, O. W.; Sandström, B., A novel dual radio- and stable-isotope method for measuring calcium absorption in humans: comparison with the whole-body radioisotope retention method12. *The American Journal of Clinical Nutrition* **2003,** *77*, (2), 399-405.
24. Plant, J. A.; Smith, B.; Phoon, X.; Ragnarsdottir, K. V., Radioactivity and radioelements. *Pollutants, Human Health and the Environment: A Risk Based Approach* **2011**, 115-146.
25. Schultz, T. W.; Kennedy, J. R., The fine structure of the digestive system of *Daphnia* pulex (Crustacea: Cladocera). *Tissue Cell* **1976,** *8*, (3), 479-90.
26. Bronk, P.; Wenniger, J. J.; Dawson-Scully, K.; Guo, X.; Hong, S.; Atwood, H. L.; Zinsmaier, K. E., Drosophila Hsc70-4 is critical for neurotransmitter exocytosis in vivo. *Neuron* **2001,** *30*, (2), 475-88.
27. Frangioni, J. V., *In vivo* near-infrared fluorescence imaging. *Current opinion in chemical biology* **2003,** *7*, (5), 626-634.
28. Qin, W.; Ding, D.; Liu, J.; Yuan, W. Z.; Hu, Y.; Liu, B.; Tang, B. Z., Biocompatible nanoparticles with aggregation-induced emission characteristics as far-red/near-infrared fluorescent bioprobes for in vitro and in vivo imaging applications. *Advanced Functional Materials* **2012,** *22*, (4), 771-779.
29. Sun, Y.; Tan, Y.; Yan, D.; Gui, Y.; Luo, W.; Zhu, D.; Wang, D.; Tang, B. Z., Recent advances of AIE-active materials for orthotopic tumor phototheranostics. *Wiley Interdisciplinary Reviews: Nanomedicine and Nanobiotechnology* **2023,** *15*, (5), e1906.
30. Gui, Y.; Chen, K.; Sun, Y.; Tan, Y.; Luo, W.; Zhu, D.; Xiong, Y.; Yan, D.; Wang, D.; Tang, B. Z., Strategies for Improving the Brightness of Aggregation-Induced Emission Materials at Aggregate Level. *Chinese Journal of Chemistry* **2023**. *41*, 1249-1259.
31. De Boer, E.; Harlaar, N.; Taruttis, A., Optical innovations in surgery. *Journal of British Surgery* **2015,** *102*, (2), 56-72.
32. Hussain, T.; Nguyen, Q. T., Molecular imaging for cancer diagnosis and surgery. *Advanced drug delivery reviews* **2014,** *66*, 90-100.
33. Owens, E. A.; Lee, S.; Choi, J.; Henary, M.; Choi, H. S., NIR fluorescent small molecules for intraoperative imaging. *Wiley Interdisciplinary Reviews: Nanomedicine and Nanobiotechnology* **2015,** *7*, (6), 828-838.
34. Kim, T.; O'Brien, C.; Choi, H. S.; Jeong, M. Y., Fluorescence molecular imaging systems for intraoperative image-guided surgery. *Applied Spectroscopy Reviews* **2018,** *53*, (2-4), 349-359.
35. Sajedi, S.; Sabet, H.; Choi, H. S., Intraoperative biophotonic imaging systems for image-

guided interventions. *Nanophotonics* **2018,** *8*, (1), 99-116.
36. Xu, W.; Wang, D.; Tang, B. Z., NIR-II AIEgens: a win–win integration towards bioapplications. *Angewandte Chemie International Edition* **2021,** *60*, (14), 7476-7487.
37. Li, Y.; Hu, D.; Sheng, Z.; Min, T.; Zha, M.; Ni, J.-S.; Zheng, H.; Li, K., Self-assembled AIEgen nanoparticles for multiscale NIR-II vascular imaging. *Biomaterials* **2021,** *264*, 120365.
38. Yan, C.; Dai, J.; Yao, Y.; Fu, W.; Tian, H.; Zhu, W.-H.; Guo, Z., Preparation of near-infrared AIEgen-active fluorescent probes for mapping amyloid-β plaques in brain tissues and living mice. *Nature Protocols* **2023,** *18*, (4), 1316-1336.
39. Xie, H.; Zhang, C.; Li, T.; Hu, L.; Zhang, J.; Guo, H.; Liu, Z.; Peng, D.; Li, Z.; Wu, W., Fast Delivery of Multifunctional NIR-II Theranostic Nanoaggregates Enabled by the Photoinduced Thermoacoustic Process. *Advanced Science* **2023**, *10,* 2301104.
40. Xie, H.; Bi, Z.; Yin, J.; Li, Z.; Hu, L.; Zhang, C.; Zhang, J.; Lam, J. W.; Zhang, P.; Kwok, R. T., Design of One-for-All Near-Infrared Aggregation-Induced Emission Nanoaggregates for Boosting Theranostic Efficacy. *ACS nano* **2023,** *17*, (5), 4591-4600.
41. Pei, P.; Chen, Y.; Sun, C.; Fan, Y.; Yang, Y.; Liu, X.; Lu, L.; Zhao, M.; Zhang, H.; Zhao, D., X-ray-activated persistent luminescence nanomaterials for NIR-II imaging. *Nature Nanotechnology* **2021,** *16*, (9), 1011-1018.
42. Liu, S.; Li, Y.; Kwok, R. T.; Lam, J. W.; Tang, B. Z., Structural and process controls of AIEgens for NIR-II theranostics. *Chemical Science* **2021,** *12*, (10), 3427-3436.
43. Jiang, R.; Dai, J.; Dong, X.; Wang, Q.; Meng, Z.; Guo, J.; Yu, Y.; Wang, S.; Xia, F.; Zhao, Z., Improving image-guided surgical and immunological tumor treatment efficacy by photothermal and photodynamic therapies based on a multifunctional NIR AIEgen. *Advanced Materials* **2021,** *33*, (22), 2101158.
44. Li, B.; Zhao, M.; Zhang, F., Rational Design of Near-Infrared-II Organic Molecular Dyes for Bioimaging and Biosensing. *ACS Materials Letters* **2020,** *2*, (8), 905-917.
45. Guo, J.-m.; Makvandi, P.; Wei, C.-c.; Chen, J.-h.; Xu, H.-k.; Breschi, L.; Pashley, D. H.; Huang, C.; Niu, L.-n.; Tay, F. R., Polymer conjugation optimizes EDTA as a calcium-chelating agent that exclusively removes extrafibrillar minerals from mineralized collagen. *Acta biomaterialia* **2019,** *90*, 424-440.
46. Beck, K.; Mariani, M.; Fletcher, M.-S.; Schneider, L.; Aquino-López, M.; Gadd, P.; Heijnis, H.; Saunders, K.; Zawadzki, A., The impacts of intensive mining on terrestrial and aquatic ecosystems: A case of sediment pollution and calcium decline in cool temperate Tasmania, Australia. *Environmental Pollution* **2020,** *265*, 114695.
47. Mei, J.; Leung, N. L.; Kwok, R. T.; Lam, J. W.; Tang, B. Z., Aggregation-induced emission: together we shine, united we soar! *Chemical reviews* **2015,** *115*, (21), 11718-11940.
48. Hong, Y.; Lam, J. W.; Tang, B. Z., Aggregation-induced emission. *Chemical Society Reviews* **2011,** *40*, (11), 5361-5388.
49. Mei, J.; Hong, Y.; Lam, J. W.; Qin, A.; Tang, Y.; Tang, B. Z., Aggregation-induced

emission: the whole is more brilliant than the parts. *Advanced materials* **2014,** *26*, (31), 5429-5479.
50. Weyhenmeyer, G. A.; Hartmann, J.; Hessen, D. O.; Kopáček, J.; Hejzlar, J.; Jacquet, S.; Hamilton, S. K.; Verburg, P.; Leach, T. H.; Schmid, M.; Flaim, G.; Nõges, T.; Nõges, P.; Wentzky, V. C.; Rogora, M.; Rusak, J. A.; Kosten, S.; Paterson, A. M.; Teubner, K.; Higgins, S. N.; Lawrence, G.; Kangur, K.; Kokorite, I.; Cerasino, L.; Funk, C.; Harvey, R.; Moatar, F.; de Wit, H. A.; Zechmeister, T., Widespread diminishing anthropogenic effects on calcium in freshwaters. *Scientific Reports* **2019,** *9*, (1), 10450.
51. Tan, Q.-G.; Wang, W.-X., Interspecies differences in calcium content and requirement in four freshwater cladocerans explained by biokinetic parameters. *Limnology and Oceanography* **2010,** *55*, (3), 1426-1434.
52. Azan, S. S.; Arnott, S. E., The impact of calcium decline on population growth rates of crustacean zooplankton in Canadian Shield lakes. *Limnology and Oceanography* **2018,** *63*, (2), 602-616.
53. Ashforth, D.; Yan, N. D., The interactive effects of calcium concentration and temperature on the survival and reproduction of *Daphnia* pulex at high and low food concentrations. *Limnology and Oceanography* **2008,** *53*, (2), 420-432.
54. Betini, G. S.; Roszell, J.; Heyland, A.; Fryxell, J. M., Calcium interacts with temperature to influence *Daphnia* movement rates. *Royal Society Open Science* **2016,** *3*, (12), 160537.
55. Tan, Q. G.; Wang, W.-X., The regulation of calcium in *Daphnia magna* reared in different calcium environments. *Limnology and Oceanography* **2009,** *54*, (3), 746-756.
56. Schultz, T. W.; Kennedy, J. R., The fine structure of the digestive system of *Daphnia* pulex (Crustacea: Cladocera). *Tissue and Cell* **1976,** *8*, (3), 479-490.
57. Gillis, P. L.; Chow-Fraser, P.; Ranville, J. F.; Ross, P. E.; Wood, C. M., *Daphnia* need to be gut-cleared too: the effect of exposure to and ingestion of metal-contaminated sediment on the gut-clearance patterns of *D. magna*. *Aquatic Toxicology* **2005,** *71*, (2), 143-154.
58. Aliberti, M. A.; Allan, E.; Bauer, D. J.; Beagen, W.; Bradt, S. R.; Carlson, B.; Carlson, S. C., An-Image-based Key to the Zooplankton of North America, Version 5.0. *University of New Hampshire Institute for Freshwater Biology* **2013**.
59. Arnott, S. E.; Azan, S.; Ross, A., Calcium decline reduces population growth rates of zooplankton in field mesocosms. *Canadian Journal of Zoology* **2017,** *95*, (5), 323-333.
60. Takvam, M.; Wood, C. M.; Kryvi, H.; Nilsen, T. O., Ion transporters and osmoregulation in the kidney of teleost fishes as a function of salinity. *Frontiers in Physiology* **2021,** *12*, 664588.
61. Byrnes, I., Rossbach, L. M., Jaroszewicz, J., Grolimund, D., Ferreira Sanchez, D., Gomez-Gonzalez, M. A., Lind, O. C., Synchrotron XRF and histological analyses identify damage to digestive tract of uranium NP-exposed Daphnia magna. *Environmental Science & Technology* **2023**, *57,* (2), 1071-1079.

753 62. Van Der Zande, M.; Kokalj, A. J.; Spurgeon, D. J.; Loureiro, S.; Silva, P. V.; Khodaparast,
754 Z.; Drobne, D.; Clark, N. J.; Van Den Brink, N. W.; Baccaro, M., The gut barrier and the fate
755 of engineered nanomaterials: a view from comparative physiology. *Environmental Science:*
756 *Nano* **2020,** *7*, (7), 1874-1898.
757 63. Cauchie, H. M.; Joaquim-Justo, C.; Hoffmann, L.; Thomé, J. P.; Thys, I., A note on the
758 use of fluorescently labelled algae for the determination of gut passage time in Bosmina and
759 *Daphnia*. *SIL Proceedings* **2000,** *27*, (5), 2987-2991.
760 64. Rivero Arze, A.; Mouneyrac, C.; Chatel, A.; Manier, N., Comparison of uptake and
761 elimination kinetics of metallic oxide nanomaterials on the freshwater microcrustacean
762 Daphnia magna. *Nanotoxicology* **2021,** *15*, (9), 1168-1179.
763 65. Tan, L. Y., Huang, B., Xu, S., Wei, Z. B., Yang, L. Y., & Miao, A. J., TiO2 nanoparticle
764 uptake by the water flea Daphnia magna via different routes is calcium-dependent.
765 *Environmental Science & Technology* **2016**, *50,* (14), 7799-7807.
766 66. Powers, E. B., The Relation between pH and Aquatic Animals. *The American Naturalist*
767 **1930,** *64*, (693), 342-366.
768 67. Pu, F.; Chen, N.; Xue, S., Calcium intake, calcium homeostasis and health. *Food Science*
769 *& Human Wellness* **2016,** *5*, (1), 8-16.
770 68. Bronner, F., Mechanisms of intestinal calcium absorption. *Journal of Cellular*
771 *Biochemistry* **2003,** *88*, (2), 387-93.
772 69. Bonjour, J. P., Nutritional disturbance in acid-base balance and osteoporosis: a hypothesis
773 that disregards the essential homeostatic role of the kidney. *British journal of nutrition* **2013,**
774 *110*, (7), 68-77.
775 70. Harvey, J. A.; Zobitz, M. M.; Pak, C. Y., Dose dependency of calcium absorption: a
776 comparison of calcium carbonate and calcium citrate. *Journal of Bone and Mineral Research*
777 **2020,** *3*, (3), 253-258.
778 71. Ahn, T.-Y.; Park, H.-J.; Kim, J.-H.; Kang, J.-C., Effects of antioxidant enzymes and
779 bioaccumulation in eels (Anguilla japonica) by acute exposure of waterborne cadmium.
780 *Fisheries and Aquatic Sciences* **2020,** *23*, (1), 1-10.
781 72. Castaldo, G.; Nguyễn, T.; Town, R.; Bervoets, L.; Blust, R.; De Boeck, G., Common carp
782 exposed to binary mixtures of Cd (II) and Zn (II): A study on metal bioaccumulation and ion-
783 homeostasis. *Aquatic Toxicology* **2021,** *237*, 105875.
784 73. Tan, Q. G.; Wang, W. X., The influences of ambient and body calcium on cadmium and
785 zinc accumulation in Daphnia magna. *Environmental Toxicology and Chemistry: An*
786 *International Journal* **2008,** *27*, (7), 1605-1613.
787 74. Meyer, J. S.; Ranville, J. F.; Pontasch, M.; Gorsuch, J. W.; Adams, W. J., Acute toxicity of
788 binary and ternary mixtures of Cd, Cu, and Zn to Daphnia magna. *Environmental toxicology*
789 *and chemistry* **2015,** *34*, (4), 799-808.
790